# Systematic method optimisation approach for small molecule imaging on the SELECT SERIES MALDI MRT - Drug mapping in fingerprints, a case study

KRISHNA, Rohith, LANGRIDGE, James, CLAUDE, Emmanuelle, BRADSHAW, Robert <http://orcid.org/0000-0003-1533-2166>, COLE, Laura <http://orcid.org/0000-0002-2538-6291> and FRANCESE, Simona <http://orcid.org/0000-0002-1381-1262>

Analytica Chimica Acta 1354 (2025) 343998

Contents lists available at ScienceDirect

Analytica Chimica Acta

journal homepage: www.elsevier.com/locate/aca

# Systematic method optimisation approach for small molecule imaging on the SELECT SERIES MALDI MRT - Drug mapping in fingerprints, a case study

Rohith Krishna [a], James Langridge [b], Emmanuelle Claude [b], Robert Bradshaw [a], Laura Cole [a], Simona Francese [a,*]

[a] Centre for Mass Spectrometry Imaging (The Sheffield Multimodal Imaging Centre), Biomolecular Sciences Research Centre, Sheffield Hallam University, Sheffield, UK
[b] Waters Corporation, Wilmslow, UK

## HIGHLIGHTS

- A systematic method development workflow is now available for small molecule imaging on new mass spectrometry technology.
- The method developed on one pair of antipsychotic/metabolite species, has shown transferability.
- For the first time, antipsychotics and their metabolites have been imaged together by MALDI MSI in a fingerprint.

## GRAPHICAL ABSTRACT

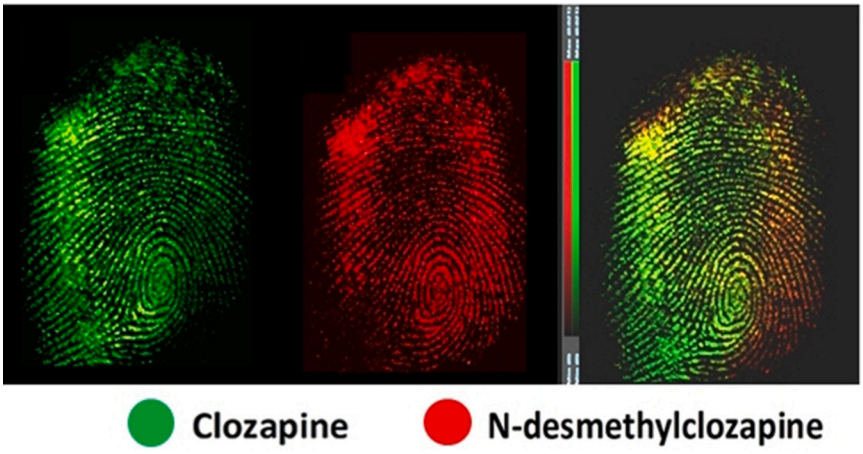


## ARTICLE INFO

Handling Editor: Dr. L. Liang

*Keywords:*
MALDI-MSI
SELECT SERIES MRT
Fingerprints
Antipsychotics
Forensic science

## ABSTRACT

Molecular fingerprinting via Matrix Assisted Laser Desorption Ionisation time-of-flight Mass Spectrometry profiling (MALDI MSP) and Imaging (MALDI-MSI) has been proven to provide biometric and lifestyle information from a fingermark. As such, it can be an effective tool to assist police investigations, thus justifying continued effort to improve the quality and range of the forensic intelligence that it is possible to provide. We are currently exploring the advancements in molecular fingerprinting capabilities on the state-of-the -art SELECT SERIES MALDI-MRT mass spectrometer based on its high mass measurement accuracy (sub-ppm) and spatial resolution (15 μm). The unique nature of this instrument requires careful optimisation to maximise the system's performance for the imaging of small molecules in fingerprints. In this study, a systematic approach to setting optimisation including optimisation of laser parameters, source voltage, quadrupole MS profile, and Transfer gas

This article is part of a special issue entitled: Imaging Mass Spectrometry published in Analytica Chimica Acta.

* Corresponding author.
*E-mail address:* s.francese@shu.ac.uk (S. Francese).

https://doi.org/10.1016/j.aca.2025.343998
Received 6 November 2024; Received in revised form 3 March 2025; Accepted 30 March 2025
Available online 1 April 2025

as well as RF voltage settings were determined for the analysis of latent fingerprint imaging and antipsychotics-contaminated fingerprint imaging. The developed method eventually yields significant improvement in image resolution over the default parameters.

## 1. Introduction

The number of applications employing MALDI-MSI has grown substantially, since its first reports in 1994 [1] and 1997 [2], due to technological improvements in sample preparation, mass spectrometry instrumentation and software processing and visualisation. The research and knowledge generated using this technique, on its own or in combination with others in multi-modal approaches, has impacted a variety of lifescience fields including, for example, biomedical (disease research and diagnostics), pharmaceuticals (drug discovery and development) and forensics (fingermark and hair imaging). The scale of application is probably due to the versatility of MALDI-MS in the analysis of small to high molecular weight compounds from drugs, lipids, amino acids to peptides, proteins and polymers, and its extended dynamic range compared to other ionisation techniques. Whilst Desorption Electrospray Ionisation Mass Spectrometry (DESI-MS) is rapidly gaining *momentum* in the imaging field to date, MALDI still currently comprises the majority of the mass spectrometry imaging experiments.

The growth in MALDI MSI applications and the depth of knowledge achieved are supported by tremendous technological efforts to improve specificity (mass accuracy and resolution), sensitivity, speed and imaging spatial resolution, which have enhanced the (accurate and comprehensive) understanding of the molecular location-function relationship.

In recent years, the most significant commercially instrumental developments have been delivered by Bruker Daltonik (TimsTOF series, with MALDI-2), Waters Corporation (SELECT SERIES MRT and Cyclic Ion Mobility) and Thermo (The Orbitrap series).

Mass spectrometers used for MSI studies have typically been axial TOF systems (either linear or reflectron instruments), or orthogonal TOF systems and, in this light, Bruker Daltonik, first to lead the way, and Waters Corporation are the two major drivers of MALDI MSI solutions, with Shimadzu offering MALDI MSI solutions for routine applications where high sensitivity, mass accuracy and spatial resolution are unnecessary.

Ion mobility significantly enhances imaging capabilities and Waters were first to commercialise ion mobility-mass spectrometry using traveling wave ion mobility (TWIMS) in stacked ring ion guides on the SYNAPT mass spectrometer [3,4]. A continued development of this technology led to the Cyclic Ion Mobility (cIM) mass spectrometer [5] which combines the cyclic ion mobility separation with enhanced performance time-of-flight mass spectrometry, offering improved sensitivity, resolution (100,000 FWHM) and mass accuracy (low ppm). The instrument was initially based on the Waters SYNAPT G2-Si IM-MS platform [5], upon modification of the separation region to slot a cyclic ion mobility (cIM) device. This region consists of a 98 cm path length, closed-loop traveling wave (TW)-enabled IM separator. The device can perform single and multi-pass separations of the ions around the cIM, whilst ejecting ions (un-acquired) outside the desired mobility, in a way that the user can control and optimise, in real time, the mobility resolution. However, currently, imaging applications are here possible only coupling the cIM with DESI.

Bruker's recently introduced trapped ion mobility spectrometry [6,7] implemented on the imaging instrument, the MALDI-2 -TimsTOF FleX, affords unprecedented sensitivity for small molecules and very high spatial resolution, down to 5 μm when MALDI-2 is combined with microGrid Technology [8–12], enabling metabolic imaging at single cell level. The first laser has a variable repetition rate of up to 10 KHz allowing for fast imaging applications. Scan speed can reach 20 pixels/s and the platform can achieve mass resolution of 60,000 at Full sensitivity resolution (FSR) at $m/z$ of 1222, and a sensitivity between 800 ppb and 2 ppm depending on the use of an internal or external calibrant respectively. The addition of ion mobility via Trapped Ion Mobility, TIMS, further improves access to detection and imaging of additional species, including those having exact masses but different mobilities. Here, a gas flow propels the ions through the TIMS tunnel. When the single ion experiences the gas flow push matching the applied electric field, it is prevented from moving beyond a position defined by its mobility. Ramping down the force of the electrical field determines the selective release of the ions from the TIMS tunnel according to their mobility.

An additional cutting edge technology for mass spectrometry imaging applications is the Waters MRT; this mass spectrometer, which can be coupled with both the DESI and the MALDI source, is a hybrid quadrupole dual orthogonal acceleration multi-reflecting time-of-flight mass spectrometer [13]. The system incorporates a universal ion source, followed by the quadrupole (MS1), stacked ring ion guide transfer optics, collision cell and transfer to the MRT analyser (MS2). The MRT analyser has a folded geometry with ions transmitted into the gridless ion mirrors via the dual orthogonal accelerator. A series of 23 periodic lenses minimizes beam divergence in the z-direction, and the resulting 46 reflections results in an ion flight path of ~47 m. The MRT offers increased mass resolution and mass accuracy which, nominally, are in the parts-per-billion range and 200,00 FWHM (300,000 in multi-pass resolution enhancement mode (REM)) respectively, independent of the acquisition speed [13]. The Encoded Frequency Pushing (EFP) algorithm establishes a threshold below which any signal that is not present in a given number of scans, and at a certain intensity, is effectively cut off; this way the algorithm not only contributes to improving mass resolution but also, together with acquisition scan speed (up to 10 pixel/s), to improved MSI applications through enhanced image clarity, in a shorter time. Lateral resolution on the MRTs can nominally reach 15 μm in MALDI mode. The MALDI source on the MRT mass spectrometer has been improved for MALDI imaging applications, compared with the MALDI source on the SYNAPT G2-Si, as described by Barré et al. [14]. In brief, the MALDI source on the MRT is equipped with a 2.5 KHz Nd:YAG laser producing 25 nJ pulses at a wavelength of 355 nm, which can be attenuated using a system of two attenuators to adjust the laser energy on surface for optimised ionisation. The laser beam can be software focused between >130 and < 10 μm. Furthermore, acquisition speeds for MALDI imaging acquisition can be increased up to 30 scans per second using the continuous raster imaging mode when the laser beam is on, whilst the movement of the sample carrier plate is continuous and at constant speed.

The technologies briefly described here certainly empower imaging applications covering both small molecules and proteomic imaging.

However, *"responsibility" is not the only thing that comes with "power"*. Such powerful instrumentation encompasses sophisticated laser and optics geometries, mass analyser combinations, auxiliary gases and even decoding algorithms. This occurrence inherently brings a significant layer of operational complexity in eventually identifying the best MSI settings/method to achieve the aims intended for a given application. This has been the case for our group when operating the first SELECT SERIES MALDI MRT delivered in the UK. The deep understanding of the instrument behaviour and response to the different parameters that could or must be set was a very time-consuming (though rewarding) process.

We acknowledge that the most widespread instrument configurations for MALDI MSI are q-TOFs (though with increasing numbers of q-Orbitraps) and that the MRT is new technology. However, the significant

increase in mass resolution and mass accuracy afforded by this technology supports a reasonable prediction that more and more of these instruments will, in time, populate mass spectrometry laboratories. In this light, we hereby intend to provide the community with a method development framework for small molecule imaging on the SELECT SERIES MALDI MRT, recently acquired at the Centre for Mass Spectrometry Imaging (CMSI) at Sheffield Hallam University. To speed up research and method development for other researchers on this state-of-the art mass spectrometer, a systematic approach is described and explained to rapidly make sense of the different options available and test settings in a logical and ordered manner.

To accomplish this aim we have had to select a "case study" and elected "molecular fingerprinting" via drug imaging as an application example.

"Molecular fingerprinting" via MALDI MSI (intended here as chemical imaging of fingermarks, ridge impressions are accidently deposited, e.g. non-deliberately generated, or of fingerprints, when the ridge impression is deliberately provided) has been clearly emerging as a powerful tool to provide biometric and chemical intelligence from fingermarks [15,16]. It has been recognised by policing nationally and internationally with the commission of the analysis of crime scene marks. It has also been recognised by the Home Office UK and the Defence Science and Technology Laboratory (Dstl, UK) with the inclusion of this technique in the international reference Fingermark Visualisation Manual, as category C in 2014 [17], and then promoted to Category B in 2023 [18], due to the increased operational character.

Given its uptake and recognition, drug imaging, an important aspect of molecular fingerprinting, makes it for a good "case study" in this paper. Also, as the method can be easily extended to drug imaging in other specimens and thus impact a number of other applications and fields of interest.

The ability to visualise drug distribution in fingermarks can provide an important link between the biometric information (ridge pattern, identifying the individual) and contextual information relating, for example, to suspect's activities prior to depositing the fingermark. The presence and distribution of the drug metabolite may indicate consumption rather than handling, which is information that may not be readily accessible to the investigators if the suspect is apprehended outside the half lifetime of the drug/metabolite. Current efforts in our laboratory aim to expand the range of illicit drugs, medications and their metabolites that is possible to detect and image in fingermarks, taking stock from the work on drug imaging via MALDI MSI reported by our group and others [19–22].

In this study, we report the development of a MALDI MSI method on the SELECT SERIES MRT to map the antipsychotic medication clozapine and its main metabolite *N*- desmethyl clozapine, in a physiological ratio and abundance, in a doped fingermark. The eventually optimised method has been successfully applied to simultaneously image the distribution of these species in a fingerprint, in amounts as low as 1.9 ng/mm$^2$, whilst contextually delivering biometric information. The method was "validated" on another antipsychotic (quetiapine) and its metabolite (7-hydroxyquetiapine) to demonstrate versatility and extendibility of the method.

As such, this paper must be taken as *(i)* an effort to provide a small molecule MALDI MS imaging method development framework on an advanced and state-of-the-art instrument, likely to be used by more and more mass spectrometry laboratories in the next few years and *(ii)* a general and logical framework of imaging method development, underpinned by the fundamental knowledge of the different mass spectrometry parameters, settings and instrumental parts.

## 2. Materials and methods

The fingerprint imaging experiments reported in this study have been undertaken following ethics approval ER60882966 granted by the Biosciences and Chemistry Department Ethics Committee at Sheffield Hallam University.

### 2.1. Materials

Ultra-pure methanol and acetonitrile (Cat 2) were sourced from ROMIL, UK Ltd. The Milli-Q water was obtained from in-house Millipore water purification system (Merck KGaA, Darmstadt, Germany). The MALDI matrix α-CHCA (Cat 1, 1 A, 1 B), Red phosphorus (Cat 2, 3), trifluoroacetic acid (Cat 1, 1 A, 3) and the standards for clozapine (Cat 3), *N*-desmethylclozapine (Cat 2, 3, 4), Quetiapine hemifumarate (Cat 1, 4), 7-hydroxyquetiapine (Cat 1,2,3), were sourced from Merck Life Science, UK Ltd. Double-sided conductive carbon tape was purchased from TAAB (Aldermaston, UK). ALUGRAM SIL G/UV254, silica precoated aluminium sheets were purchased from Macherey-Nagel GmbH, Germany.

### 2.2. Instrumentation, data acquisition and data processing

Spray-coat matrix deposition was performed on the HTX M3+ Sprayer™ (HTX Imaging, North Carolina, USA). The MALDI measurements were performed on the multi-reflecting QToF SELECT SERIES™ MRT (Waters Corp., Wilmslow, UK) incorporating a 2.5 kHz solid state Nd:YAG laser at a repetition rate of 1 KHz, utilizing a 50 μm step size at a scan rate of 0.2 s, and operated in positive ion mode, within the instrument operating between *m/z* 50 and 2400. Data acquisition was conducted using MassLynx™ v4.2 and the Quartz v2.7.1 software. All imaging experiments were continuous lockmass corrected (CLMC) during acquisition using the α-CHCA ion at *m/z* 212.03233 (included within the instrument method file). The instrument was calibrated prior to every analysis using phosphorus red to achieve sub-ppm levels mass accuracy in the *m/z* 50–2400 mass range. The laser intensity (LI), lens focus (LF) and functions of the secondary attenuator (SA) were primarily optimised followed by the tuning and evaluation of the sample plate voltage (SPV) and extraction voltage (EV) effects. The quadrupole profile optimisation and then the transfer RF optimisation were finally undertaken to target specific *m/z* ranges and achieving higher sensitivity. Aside from laser tuning and source parameter comparison for which fingerprints of 2 × 2 mm and 6 × 6 mm in size were used, fingerprint regions of 1 × 1 mm in size were employed for the source voltages, gas flow, quadrupole profile and RF optimisations.

*EFP Mode Selection* **-**The decoding algorithm mode can be selected in the method file prior to analysis. The two available options are automatic and low threshold mode (see Supplementary Fig. S1(i)).

*Laser Optimisation* **-** Laser intensity and lens focus parameters were varied in the 'MALDI source' window in the software (supplementary Fig.S1(ii)), from 200 to 350 and from 3 mm to 8.5 mm, respectively; the secondary attenuation was also optimised. The ions at *m/z* 299.30692 and *m/z* 304.30057 were used as qualifiers for the laser optimisation. The latter ion is an external contaminant, common antibacterial dodecylbenzydimethyllammonium ion [23] detected with a mass accuracy of 0.49 ppm. The ion at *m/z* 299.30692 could not be putatively identified in LipidMaps (in lipidmaps.org). However, the identity of either of these two ions is unimportant as for biometric purposes, they simply serve the scope of appropriately reconstruct the ridge pattern of the fingerprint. The effects of the laser repetition rate were also studied by varying this from 100 Hz up to 2000 Hz.

*Source Parameter Optimisation* - The sample plate voltage and the extraction voltage were primarily investigated and varied in the 'MALDI' source window in the software (supplementary Fig. S1(ii)) between 0-50 V and 10–50 V, respectively. The effect of MALDI gas ($N_2$) flow was studied by varying the flow rates from 100 mL/min up to 400 mL/min.

*Quadrupole RF Profile Optimisation* **-** The quadrupole RF profiles were studied, specifically the effect of the automatic profile, manual fixed profile (mass A = *m/z* 100, *m/z* 500, and *m/z* 800), and manual profile (mass A = *m/z* 250, mass B = *m/z* 300, mass C = *m/z* 400), using

fingerprint regions. The sensitivity comparison experiments between the three profiles were undertaken using fingerprints spotted with clozapine standard spotted in a ten-fold serial dilution from 1000 ng/mL – 1 ng/mL. The quadrupole RF profile selection was carried out through the software under the 'Quad/MS profile/DRE' window (see supplementary Fig.S1(iii)).

*Transfer RF Optimisation* - The transfer RF voltages, transfer collision gas as well as the transfer RF gain were studied utilizing latent fingerprint regions and clozapine-spotted fingerprints to optimise transmission. Transfer RF voltages of 150, 500 and 800 V were investigated. The transfer collision gas ($N_2$) was also tested by varying the flowrates from 1 mL/min to 1.7 mL/min. Finally, the transfer RF gain was optimised from the arbitrary gain values of 1 up to 5 on clozapine-spotted fingerprints with clozapine concentrations varying from 100 to 1 ng/mL in a ten-fold serial dilution. All the RF voltage selections were manually made through the software under the 'RF' window (see supplementary Fig S1(iv)), and the transfer collision gas values were changed under the 'Transfer' window (see Supplementary Fig. S1(v)).

For data processing, all the raw data were initially processed and visualised in HDI™ 1.7 (Waters Corporation, Wilmslow UK), with the following parameters: MS resolution of 200,000, *m/z* window of 0.005 Da, and the number of most intense peaks set to 1000. All the images were TIC (Total Ion Count) normalised, except for the EFP mode selection experiment to avoid image artefacts due to the variation in TIC. In TIC normalisation, the systematic artefacts in the mass spectral intensity are removed by dividing the intensity value of each peak, by the sum of all peak intensities in that particular pixel. Relevant regions of interests (ROI) were exported to MassLynx™ v4.2 software for spectral interrogation.

### 2.3. Sample preparation

Drug-contaminated fingerprints and drugs/metabolites were deposited/spotted on silica-removed aluminium sheets which were secured to the MALDI target plate (Waters Corp. Wilmslow, UK) using double-sided carbon tape prior to MALDI analysis. For fingerprint drug spotting experiments, ungroomed fingerprints were generated as previously described [24]. All the optimisation experiments were carried out on the same fingerprint sample to reduce variation. Both optimisation and validation experiments employed the fingerprint from different digits from the same person only. No other donors were recruited. The drug and metabolite standard solutions in methanol were prepared in a concentration range between 1000 ng/mL to 0.1 ng/mL in a ten-fold dilution series. For imaging of spotted drugs, drugs/metabolites were mixed with α-CHCA in 70:30 v/v ACN:0.1 % $TFA_{aq}$ in a 1:1 ratio and 0.5 μL of the resulting solutions were spotted on groomed fingermarks for optimisation and sensitivity experiments. These experiments were repeated twice for clozapine and *N*-desmethylclozapine. Drug and metabolite-contaminated ungroomed fingerprints were prepared according to the method previously reported by Groeneveld et al. [19] to ensure homogeneity across the sample, while employing two drugs and their main metabolites namely clozapine and *N*-desmethylclozapine and quetiapine hemifumarate and 7-hydroxyquetiepine. Briefly the drugs and their metabolites, each at a concentration of 10 μg/mL were mixed in a 1:1 ratio and 50 μL of the resulting solution were spotted on to a pre-cleaned glass microscope slide. The solvent was allowed to evaporate under ambient conditions. The fingertip was dragged side-to-side to transfer as much of the drug and metabolite on to the fingertip as possible. The fingertip was then contacted with a cleaned aluminium sheet, to produce drug and metabolite-contaminated ungroomed mark. These experiments were repeated twice for the clozapine/*N*-desmethylclozapine mixed solution.

### 2.4. Matrix deposition for imaging experiments

Samples were coated with 8 layers of 5 mg/mL α-CHCA prepared in 70:30 ACN:0.1 % $TFA_{aq}$. Following optimisation, the M3+ sprayer (HTX Technologies, US) was operated with a nozzle temperature of 75 °C, pressure of 10 psi, flowrate of 100 μL/min and a velocity of 1200 mm/min.

## 3. Results and discussion

This study aims to investigate the operational parameters that enable technological and instrumental advances implemented within state-of the-art MSI-enabled MRT mass spectrometers. In particular, a workflow is described to systematically and logically develop a method to image small molecule on the SELECT SERIES™ MALDI MRT that leads to optimal sensitivity and image clarity (within a 50 × 50 μm spatial resolution settings). To illustrate the workflow and the impact of the different settings, drug imaging in fingerprints was employed as a case study. Specifically, clozapine, an antipsychotic, and its main metabolite *N*-desmethylclozapine were selected for this work because clozapine is *(i)* a commonly administered antipsychotic used mainly to treat schizophrenia (and can be effective in bipolar disorders too) [25], *(ii)* already known to be physiologically excreted in sweat and detectable in patients' fingerprints when taken in therapeutic doses [26] and *(iii)* known to be amenable to MALDI MS and MSI [27,28].

The method underwent systematic development and optimisation starting with the laser intensity (LI), laser focus (LF) and functions of the secondary attenuator (SA) tuning, followed by the investigation of the sample plate voltage (SPV) and extraction voltage (EV) effects. To boost sensitivity, the subsequent step encompassed the identification of the optimal quadrupole profile, whilst tuning of the transfer RF additionally impacted image clarity. All the imaging experiments were continuous lock mass corrected (CLMC) during acquisition, using the sodiated α-CHCA ion signal at *m/z* 212.03233 This is an important step in achieving optimal performance of mass spectrometer and Supplementary figure Fig. S2 illustrates the difference in the quality of the fingerprint images with and without CLMC.

Encoded Frequency Pushing (EFP) is a spectral multiplexing technique that improves the duty cycle of long flight time MRT analysers. The EFP algorithms have been described in detail, but the demultiplexing of this data is performed in a graphics processor unit (GPU) [29] with the user having access to a single threshold. This threshold enables the number of non-zero spectra that are allowed for an ion to pass the intensity to be varied by choosing between the "low thresholding" and the "default automatic setting" only. This selection very much depends on the type of experiment being conducted, which, in this case study, are the MALDI-MSI of small fingerprint regions (1 × 1 mm and 2 × 2 mm), for method development, or an entire fingerprint sample (approximately on average 20 × 10 mm) for a "targeted" imaging analysis. The overall approach for the optimisation of the method for fingerprint and drug-contaminated fingerprint imaging on the SELECT SERIES™ MALDI-MRT is depicted in Fig. 1 flowchart and each parameter will be discussed in the next sections, following the order in the flowchart.

*Encoded frequency pushing (EFP) algorithm mode selection* - The decoding algorithm mode can be selected in the method file prior to analysis. In EFP mode, the MALDI-MRT instrument acquires data with an encoded x128 pulse pattern to improve the duty cycle from the long flight time TOF (2 msec for *m/z* 2400). The data acquired using this 128-pulse pattern is subsequently decoded algorithmically in a GPU. The EFP algorithm provides decoded data that has reduced image noise leading to reduce data size and hence significantly enhances image clarity. It is configured to allow for the selection of two thresholds, automatic and low threshold respectively.

In order to have a direct comparison of the effects of the EFP automatic and low threshold modes, split fingerprint imaging experiments were conducted and shown in Fig. 2.

The ridge continuity obtained through the application of the low threshold mode (Fig. 2A) is higher compared to the half fingerprint

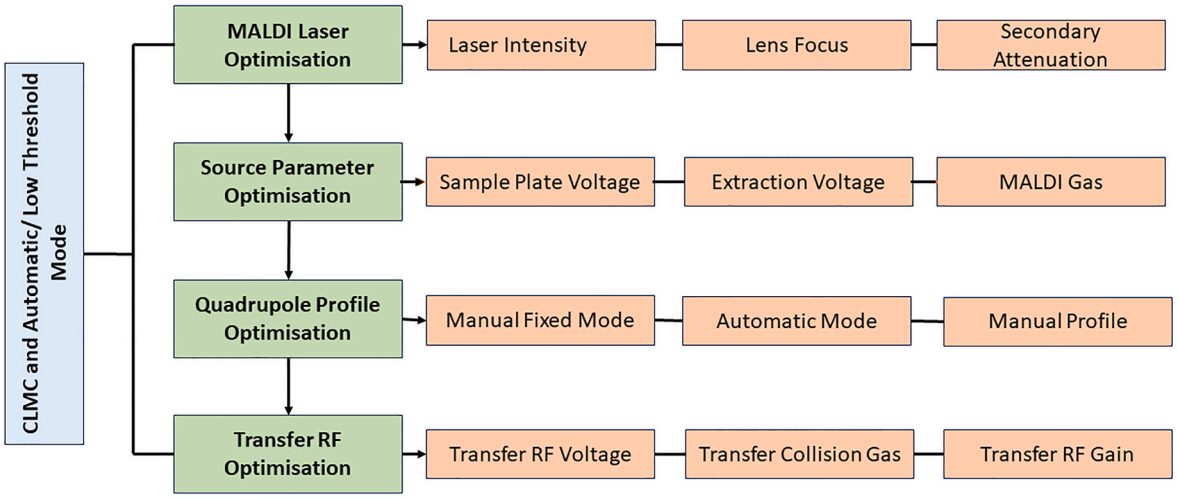


**Fig. 1.** Flowchart depicting the general systematic optimisation protocol for small molecules MALDI MSI on the SELECT SERIES™ MALDI MRT.

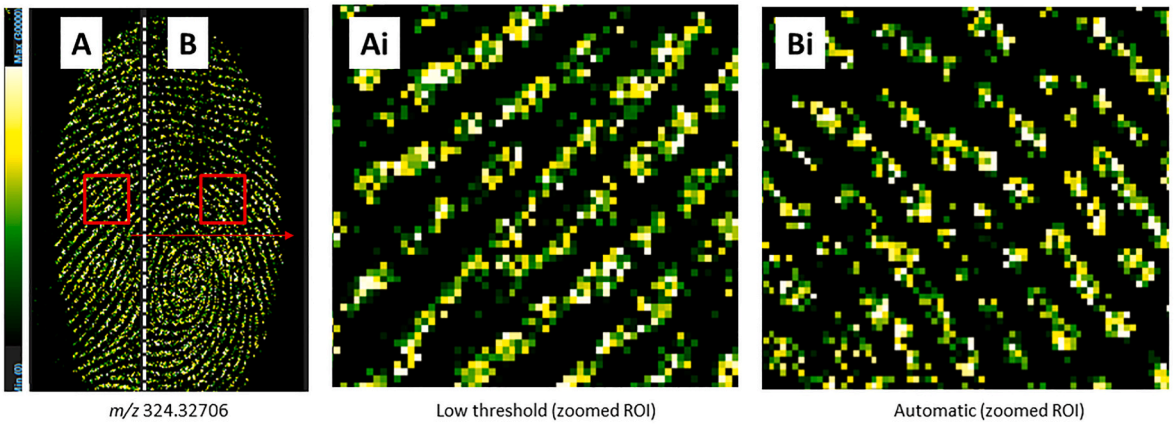


**Fig. 2.** Application of the EFP decoding algorithm in low threshold and automatic modes to a large image (20 × 10mm) at 50 μm. A representative example is shown for the ion at *m/z* 324.32706. The left-hand side of the split mark was acquired in low threshold mode (*A*) with (*Ai*) showing ridge detail in a zoomed region. The other half of the split fingerprint in automatic mode (*B*) with (Bi) showing the ridge detail in a zoomed in region. The red frame in the A-B panel shows the zoom in region selected across the splitting line, reported in (*Ai*) and (*Bi*). Here no normalisation by TIC has been applied. (For interpretation of the references to colour in this figure legend, the reader is referred to the Web version of this article.)

imaged in automatic mode (Fig. 2B). The low threshold mode has a slightly higher TIC (3.54e7), as compared to the automatic mode (2.75e7). We have elected to show the image of the ion at *m/z* 324.32706 as representative of the distribution of other ions detected in the fingerprint and because of its homogeneity of distribution on the ridges which facilitates the interpretation of the results as a direct consequence of the parameters optimisation. The image of this ion in Fig. 2B and its zoomed in inset (Fig. 2Bi) are explained by the way the algorithm operates; in automatic mode, if individual *m/z* ion signals do not meet a certain intensity threshold or are not present in a pre-determined number of scans, they are considered as "noise" and are automatically binned through the decoding process, resulting in a less full ridge detail coverage, as observed in (Fig. 2Bi). Therefore, where the biometric information depends on the ridge pattern continuity, the low threshold mode is preferred. However, in general terms, low thresholding mode generates much bigger datasets (Gb versus Mb), closer to the size of conventional qToFs.

*Laser Optimisation*- The laser tuning was performed on fingerprint regions of 2 × 2 mm in size by varying the laser intensity values, lens focus as well as enabling the secondary attenuator in order to achieve the required sensitivity and spatial resolution using α-CHCA matrix at 50 μm. It is important to note that the laser optimisation is also dependant on the pixel size, the number of shots and the matrix employed. These factors have been investigated and their effect illustrated in [30].

The laser intensity (displayed in arbitrary units; 0–500) is controlled by the primary and secondary attenuator. The primary attenuator is a variable transmission neutral density wheel, and a second fixed neutral density filter can increase the dynamic range of the primary attenuator when the laser beam is focused [30]. The lens focus changes the spot size of the laser by controlling its focal length; the laser is defocused when the focus is set to 0. Finally, the secondary attenuator is an ND filter which enables a 10-fold reduction in the intensity of the laser which provides extended dynamic range to attenuate the laser beam energy. The two-part attenuation system enables a large range of laser focusing between >130 and < 10 μm [30]. Ion signals at *m/z* 299.30692 and *m/z* 304.30057 were used as qualifiers for the laser optimisation (data not shown). Using the ion at *m/z* 299.30692, the effect of the laser repetition rate was also investigated for a small fingerprint region of 1 × 1 mm in size by varying it from 100 Hz up to 2000 Hz. A representative summary of the data obtained through tuning the laser parameters is presented in Fig. 3.

For a latent fingerprint, the best ion signal intensity and image clarity was achieved employing a laser intensity of 350 a.u. and a lens focus

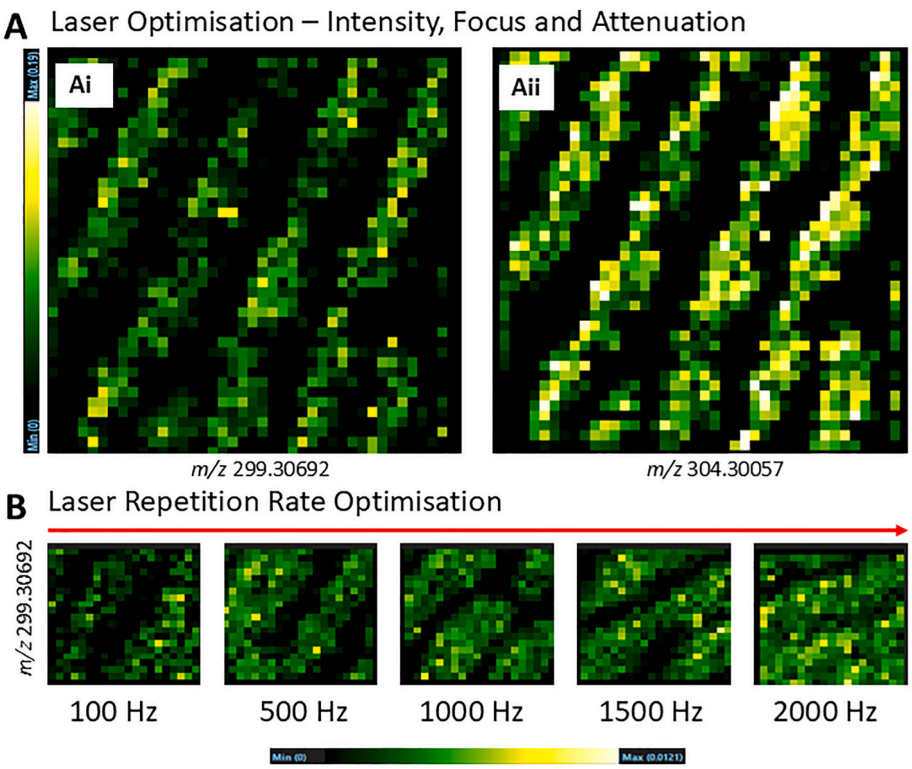


**Fig. 3.** MALDI MSI laser parameter optimisation *A:* MALDI images of the ions at *m/z* 299.30692 (*Ai*) and 304.30057 (*Aii*) obtained from a small region of a fingerprint at the optimised laser intensity (350), lens focus (6.00 mm) and secondary attenuation (ON). *B:* effect of varying laser repetition rate on signal intensity and ridge pattern quality using *m/z* 299.30692 as an example. Imaging data are normalised by TIC. Pixel size at 50 μm.

value of 6.00 mm. In the case of fingerprints, a well optimised laser parameter assists in the provision of a better ridge pattern continuity and overall image resolution.

The MRT is equipped with a 2.5 kHz laser, which provides continuous rastering capabilities. This enables faster acquisition times [14,31]. As Fig. 3B shows, increasing the laser repetition rate beyond 1500 Hz leads to a decrease in image clarity and ridge blurring/merging potentially due to arising oversampling. However, it is also possible that the laser might have been firing in areas of the MALDI plate where there was no sample left, thus generating some chemical background, and hence requiring a similar number of laser shots. The instrument is generally optimised at a laser rate of 1000 Hz for most of the MALDI profiling applications. It is still possible to work at the higher end, provided that the laser intensity (density filter energy parameter) is reduced to a lower value (100–200 range).

The sample plate and extraction voltages were set at the default values of 0 and 10 respectively for the MALDI gas flowrate optimisation.

The MALDI gas flow ($N_2$) is optimised at 350 mL/min for general imaging needs ensuring a good transfer of ions. By favouring collisional cooling, the higher flowrate ensures a higher intensity signal and hence better sensitivity [32]. Having the gas flow switched OFF or at lower rates could lead to excessive matrix and sample material build-up on the hexapole and to subsequent lower sensitivity and imaging repeatability issues. Switching off the gas flow is not recommended even though the hexapole can be easily removed for cleaning, without having to vent the MALDI-MRT due to the isolation valve engineered into the instrument. Low gas flow experiments can be considered for smaller sample sections to enhance metabolite coverage in biological specimens [33]. The hexapole cleanliness should be monitored and maintenance (actual protocol and frequency) should be reported in SOPs to maximise repeatability.

The sample plate voltage (SPV) is applied to the sample plate through a connector at the bottom-left corner of the plate holder. An increase in SPV can provide additional acceleration to the generated ions. In the case of small *m/z* ions as that at nominal *m/z* 299 in Fig. 4B, this can lead to a reduction in its intensity and eventually to complete lack of visualisation at high SPV values, whereas for larger *m/z* ions, such as that at nominal *m/z* 551 also imaged in Fig. 4B, it has, as it may be expected, the opposite effect. The extraction voltage (EV) is responsible for the extraction of the ions into the mass spectrometer and is the electric potential difference applied between the sample plate and the entrance to the mass analyser. The sample plate voltage in combination with the extraction voltage, establishes an electric field that propels the ions into the mass spectrometer [34,35]. Having a higher EV value is not always conducive to an increase in sensitivity; in fact, it can create artefacts in the images generated and therefore it requires optimisation based on the type of analytes to be imaged. In the case of small molecule imaging in fingerprints, a SPV value of 0 and an EV value of 10 are ideal (Fig. 4D). For higher *m/z* species, an SPV value of 50 and an EV value of 20 are more appropriate (Fig. 4E) provided the quadrupoles and RF values are optimised (see next sections).

*Quadrupole Profile Optimisation* - The quadrupole automatic profile, manual fixed profile (M = *m/z* 100, *m/z* 500, and *m/z* 800), and manual profile (M1 = *m/z* 250, M2 = *m/z* 300, mass M3 = *m/z* 400) were tested and optimised next and the results are presented in Fig. 5.

The MALDI MRT is equipped with a mass resolving quadrupole MS1 mass analyser with an 8 kDa resolving mass range. The quadrupole is operated in RF-only mode for MS mode analysis to transmit a wide *m/z* range. The instrument provides three distinct quadrupole profile options, namely manual fixed, automatic and manual profile. The manual fixed profile places the RF amplitude to a single set value corresponding to a given *m/z* position. The automatic mode ramps the quadrupole rectified RF voltage across the standard MRT *m/z* range 50–2400. Finally, in the manual profile mode, three *m/z* positions (M1-3), two individual dwell time (%) (D1, D2) and two ramp time (%) (R1, R2) can be set to transmit interested regions of the *m/z* range.

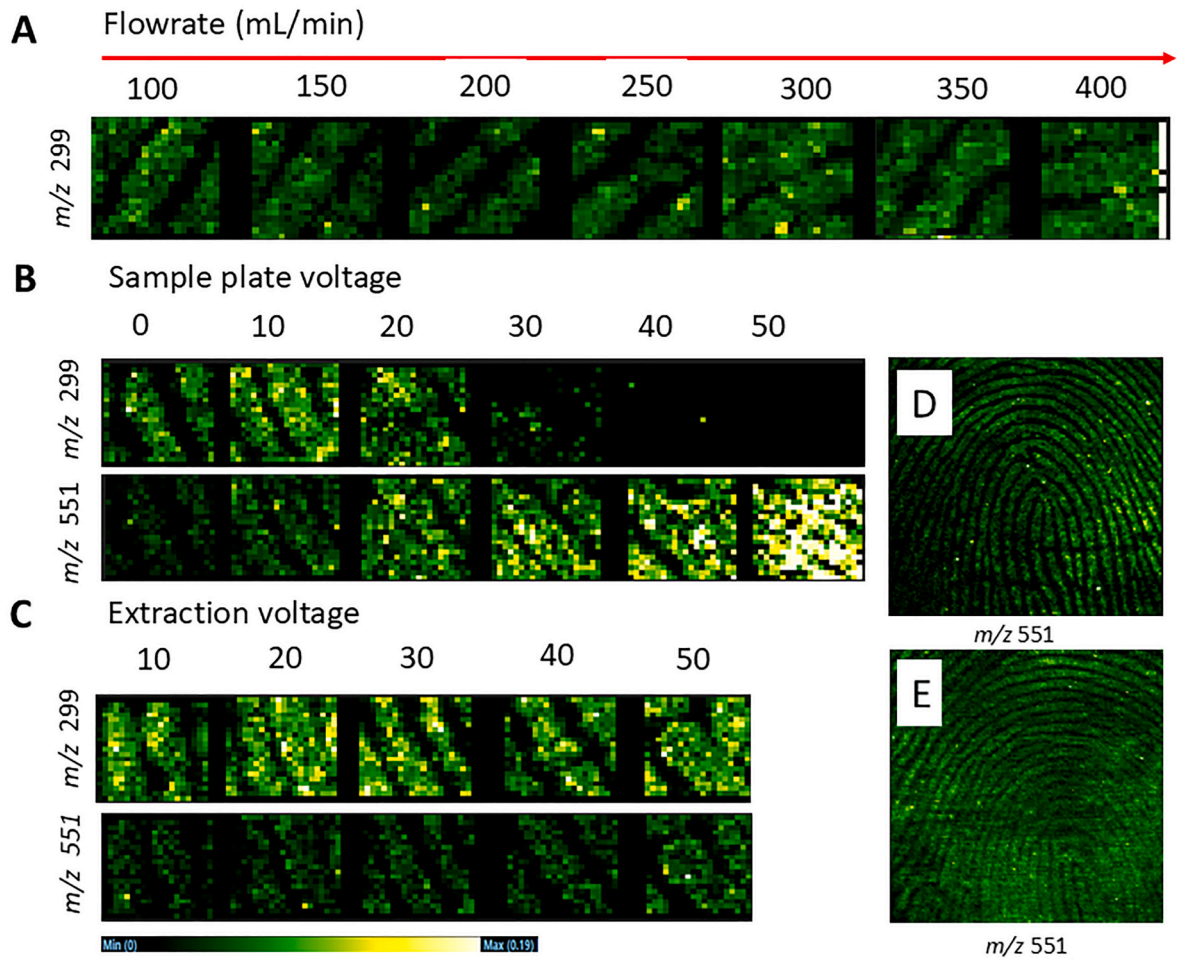


**Fig. 4.** Latent fingerprint imaging and source parameters optimisation. *A:* MALDI gas flowrate optimisation (100–400 mL/min) undertaken recalling images of the ion at *m/z* 299.30692 (nominal *m/z* 299). *B*: Sample plate voltage optimisation (0–50 V) undertaken recalling images of the ions at nominal *m/z* 299 and *m/z* 550.63031 (nominal *m/z* 551). *C*: Extraction voltage optimisation (10–50) imaging the same ions as in *B*. *D*: Fingerprint region (6 × 6 mm) imaged using SPV = 0 and EV = 10 settings showing the ion at nominal *m/z* 551 which was also imaged in *E*: Fingerprint region (6 × 6 mm) imaged using SPV = 50 and EV = 20 settings. Data is normalised by TIC. Pixel size at 50 μm.

*Source Parameters Optimisation* - The MALDI gas flowrate, the sample plate voltage and extraction voltage were primarily investigated on latent fingerprint regions of 1 × 1 mm in size. The effect of the source parameters on fingerprint images is presented in Fig. 4.

This is accomplished by dwelling at the first *m/z* position for D1 % of the time, ramp to second *m/z* position over R1 % of time, dwell at the same *m/z* for D2 % of the time and finally ramp to the third *m/z* position over R2 % of the time.

We have elected to show the images of distribution for the ions at *m/z* 299.30692, 550.63031 and 915.02545 as representative ion images to span across the *m/z* 0–1000 range of interest. As observed in Fig. 5, the automatic profile allows the entire *m/z* range to be transmitted, although a slight decrease in absolute signal intensity (>3) is observed for higher *m/z* ions when compared to fully optimised manual fixed and manual profile modes Fig. 5(C–E). The manual fixed profile is user definable, targeting a specific region of the *m/z* range according to the *set* value. This profile is ideal to specifically detect a targeted *m/z* value, or a region of interest of the *m/z* range, with optimal transmission. Experimental results, comparing the sensitivity of detection for clozapine spotted on a fingerprint in a range between 1000 ng/mL and 1 ng/mL (in a ten-fold serial dilution) using the automatic, manual fixed, and the manual profile, are presented in Fig. 6.

The quadrupole mass selection, dwell time and ramp time for the three profiles in this spotted clozapine experiment are reported in Table 1.

In Fig. 6 it can be observed that: *(i)* the selection of the automatic profile enabled the visualisation of up to 10 ng/mL of clozapine (nominal *m/z* 327) (Fig. 6A) as confirmed by the ROI average mass spectrum (data not shown); *(ii)* the manual fixed profile (Fig. 6B) (*m/z* 327) and manual profile (Fig. 6C) (M1 = *m/z* 250, M2 = *m/z* 300, M3 = *m/z* 400) enabled higher sensitivity with clear clozapine visualisation at 10 ng/mL and also visible, at lower intensity, up 1 ng/mL, as confirmed by the ROI average mass spectrum (data not shown). The automatic profile (Fig. 6A) yields a reduced relative intensity for the serially diluted clozapine spots. Upon spectral interrogation by extracting regions of interest (ROI), it was observed that the automatic profile yielded detection of clozapine also at a concentration of 1 ng/mL with a significantly lower intensity as compared to the other quadrupole profiles. The signal intensity at 1000 ng/mL was maximum for the manual fixed profile, as expected, closely followed by the manual profile, with the automatic profile yielding a significantly lower intensity for clozapine at the same concentration. These trends are illustrated in Supplementary Fig. S3.

*Transfer RF Optimisation* – The transfer collision gas pressure, the transfer RF voltages, and the transfer RF gain were tuned to achieve optimal sensitivity for clozapine-contaminated fingerprints. Fig. 7 shows the effect on small fingerprint regions, upon variation of the transfer collision gas ($N_2$) between 1 mL/min to 1.7 mL/min flowrate (Fig. 7A).

The transfer collision gas is applied directly in the transfer stacked ring ion guide and its optimisation can help improve RF-based mass

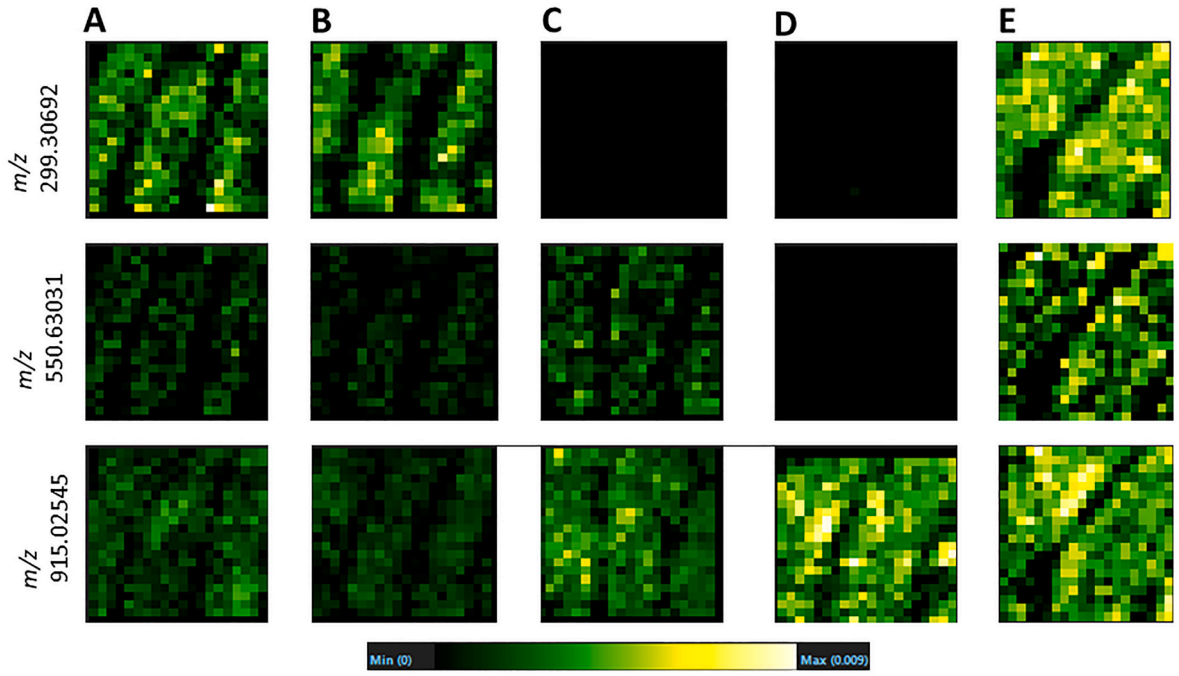


**Fig. 5.** Quadrupole profile effects on MALDI MS images of latent fingerprints. These effects were studied using representative ions at *m/z* 299.30692, 550.63031 and 915.02545 (nominal *m/z* 299, 551 and 915 respectively). *A*: automatic profile; *B, C and D:* manual fixed profile set at *m/z* 100, *m/z* 500 and *m/z* 800, respectively, and *E*: Manual profile set at *m/z* 250, *m/z* 300 and *m/z* 400. Data is normalised by TIC. Pixel size at 50 μm.

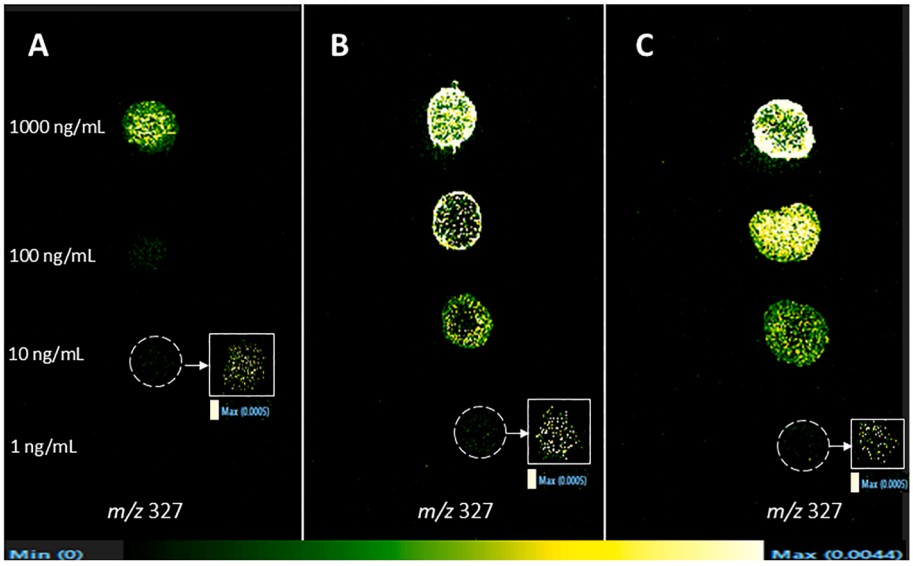


**Fig. 6.** Sensitivity afforded by the different quadrupole RF profiles applied to the MALDI MRT MSI analysis of clozapine (nominal *m/z* 327) spotted on a fingerprint. *A*: automatic profile, *B*: manual fixed at nominal *m/z* 327, and C manual profile mode set at nominal *m/z* 250, *m/z* 300 and *m/z* 400. Data is normalised by TIC. Pixel size at 50 μm.

transmission and collisional cooling. The lower gas flowrates enable smaller *m/z* ions to be effectively transmitted, as shown for the ion at nominal *m/z* 240, while increasing the flow rates favours larger *m/z* ions by providing additional collisional cooling. The default parameter is for the flow rate set at 1.2 mL/min which is ideal for broad transmission of the majority of molecular species expected to be detected in a fingerprint (particularly lipids in the 100–1000 *m/z* range). Fig. 7B–D, shows the different profile of transmitted *m/z* according to the selection of the Transfer RF voltage. Additionally, for fingerprints spotted with 1 μg/mL clozapine solution, pixel density and distribution in the corresponding images vary with different transfer RF voltages from 150 to 500, through to 800 (Fig. 7B–D). As expected and recommended, an RF voltage value of 150 is ideal for small molecules (Fig. 7Bi), as it provides a realistic distribution of the drug spotted on the fingerprints, in comparison to the RF voltage of 500 (Fig. 7Ci) which yields an image with a sharper low *m/z* cut-off (as expected) and a number of higher *m/z* species. Finally, setting the RF voltage even higher, at 800 (Fig. 7Di), yields images with a higher *m/z* cut-off (again as expected due to the transmission of RF only devices) with increased transmission of the higher *m/z* species. This behaviour is expected for an RF only stacked ring ion guide, which exhibit a sharp low *m/z* cut-off (x0.78 of the set mass) and a broad transmission of up to a decade in mass to high mass [36]. As such, the RF

**Table 1**
The quadrupole profile parameters for automatic, manual fixed and manual profile on the SELECT SERIES MRT for the MALDI MSI analysis of clozapine (nominal *m/z* 327) spotted on a fingerprint.

| | Automatic profile | Manual fixed profile | Manual profile | | |
|---|---|---|---|---|---|
| ***m/z*** | 50–2400 | 327 | 250 | 300 | 400 |
| **Dwell time (%)** | 25 | 100 | 20 (D1) | | 50 (D2) |
| **Ramp time (%)** | 75 | 0 | 20 (R1) | | 10 (R2) |

voltage should always be kept lower than the *m/z* of the ion to be transmitted. To achieve optimal sensitivity for imaging both the drug detection and imaging and endogenous compounds in the fingerprint, the transfer RF gain was further optimised from the arbitrary gain values 1–5 for fingerprints spotted with Clozapine in concentrations between 100 and 0.1 ng/mL (in a 10-fold serial dilution, with corresponding MALDI MS images shown in Fig. 7E–I. The transfer RF gain is the gradient applied to the transfer RF ramp, which is linked to the quadrupole ramp. This can affect transmission for different molecular ions, depending upon the gradient applied, combined with the optimised quadrupole and transfer RF parameters.

The gain values in the range of 1–5 were investigated. As shown in

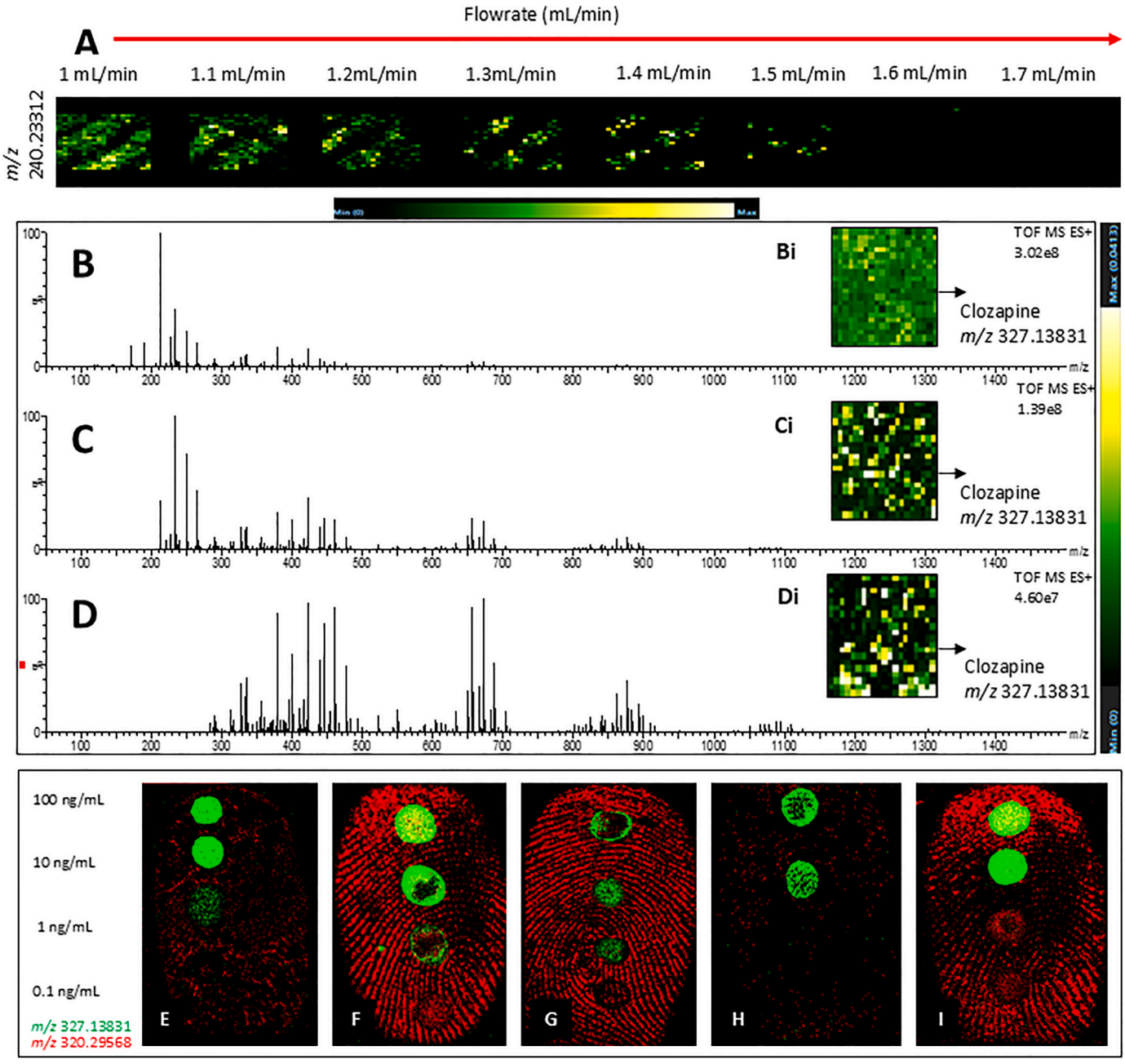


**Fig. 7.** MALDI MSI optimisation of the Transfer RF device for clozapine-spotted fingerprints, *A*: transfer collision gas optimisation varying the flow rate between 1 and 1.7 mL/min monitoring the ion at *m/z* 240.23312. *B*: transfer RF voltage of 150 on a fingermark section and (Bi) showing clozapine (1 μg/mL) spotted on the same section. *C:* transfer RF voltage of 500 on a fingermark section and (Ci) showing clozapine (1 μg/mL) spotted on the same section. *D:* transfer RF voltage of 800 on a fingermark section and (Di) showing clozapine (1 μg/mL) spotted on the same section. *E-I:* clozapine (*m/z* 327.13831) spotted from 100 ng/mL to 0.1 ng/mL overlayed with the fingerprint ion image at *m/z* 320.29568 to study the variation in sensitivity with change of transfer RF gain values from 1 to 5; respectively. Data is normalised by TIC. Pixel size at 50 μm.

Fig. 7G, the transfer RF gain value of 3 was found to be most suitable for the optimised small molecule method, maximising ion transmission for the target drug and a number of other potentially important ions within the quadrupole profile range.

### 3.1. MALDI MSI method testing

The optimised settings reported in Supplementary Table S1 and discussed in the previous section for the imaging of the small molecule range, and in particular for spotted clozapine in fingerprints, were applied to clozapine and *N*-desmethylclozapine in both spotting experiment (1000 ng/mL-0.1 ng/mL) as well as for drug-contaminated fingerprints, prepared according to Groeneveld et al. [19]. As shown in Fig. 8, specifically 8 A and 8 B, the optimised MALDI MSI method enabled the detection of clozapine down to 1 ng/mL concentration, and *N*-desmethylclozapine down to 10 ng/mL in the sensitivity experiments. In the case of the drug-contaminated fingerprints experiments (Fig. 8C–D), a 1:1 solution of the drug and metabolite was employed to eventually contaminate a fingertip and subsequently generate a fingerprint. This ratio was selected for demonstration purposes; although in 20 schizophrenic patients study by Ming and Heathcote [37], clozapine and *N*-desmethylclozapine were detected in serum at an average ratio of 1.4, the ratios varied between 0.86 and 2.2. Considering that ratios depend on individual variability, formulation and also on drug adherence, and that the average ratio in sera may not necessarily be the same in other biological fluids/specimens, we considered in our study a 1:1 ratio for simplicity. Within this experiment, both clozapine and metabolite were visualised on the ridges. The overlay of the MALDI images of clozapine and its metabolite shown in Fig. 8E improved the ridge pattern detail and continuity; as such, images in Fig. 8C–E can provide both toxicological and biometric intelligence.

In order to further demonstrate that the optimised MALDI MSI method is applicable to small molecule imaging in general within the 100–1500 *m/z* range, the method was applied to another fingerprint contaminated with a second antipsychotic drug, quetiapine hemifumarate (prescribed to patients with bipolar disorder and schizophrenia), and to its metabolite 7-hydroxyquetiepine.

The optimised MALDI MSI method enabled the visualisation of the spotted quetiapine hemifumarate (Fig. 9A), down to 1 ng/mL which is still visible within the overlaid image with an endogenous fingerprint molecule (Fig. 9A). It was also possible to visualise 7-hydroxyquetiepine down to 10 ng/mL (Fig. 9B). As for clozapine and *N*-desmethylclozapine fingerprint imaging experiments shown in Fig. 8C–E, fingerprints were also generated by contaminating a fingertip with a mixed solution of the two species. As previously, using the same rationale employed for preparing the mixed solution clozapine/*N*-desmethylclozapine, a 1:1 ratio quetiapine/7-hydroxyquetiepine was employed. The drug-contaminated fingerprint enables visualisation of both the drug (Fig. 9C) and metabolite.

(Fig. 9D). The individual MALDI-MS images for the two species have been overlaid in Fig. 9E to provide the full fingerprint image. In order to provide even better biometric information, ridge pattern continuity was improved by overlaying additional ion images from ions at *m/z* 550.63031 and *m/z* 522.59814 (Fig. 9F).

With respect to detection and quantification of clozapine, quetiapine and their metabolites, extraction and LC MS or LC MS/MS have been the

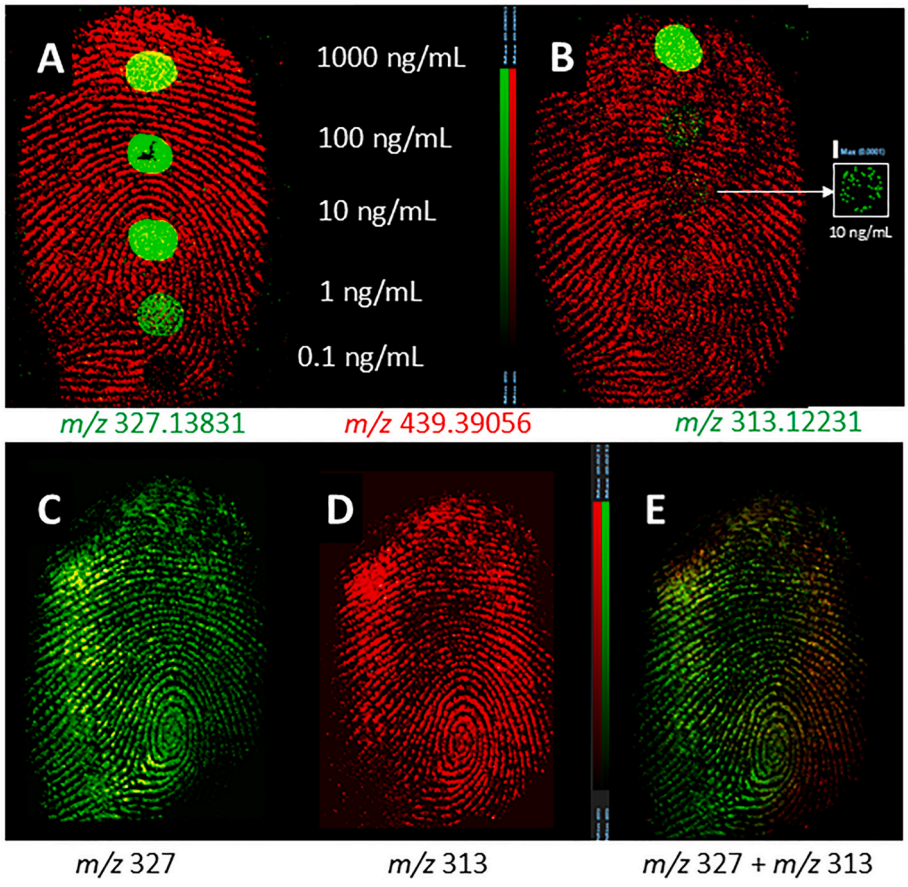


**Fig. 8.** Application of optimised small molecules MSI method for clozapine (*m/z* 327.13831) and its metabolite *N*-desmethylclozapine (*m/z* 313.12231). *A* and *B* show sensitivity test for clozapine and its metabolite by spotting them in multiple 10-fold serial dilutions between 1000 ng/mL and 0.1 ng/mL, and the fingerprint is overlayed with an ion image at *m/z* 439.39056. *C*: clozapine and *D: N*-desmethylclozapine contaminated-fingerprints, and *E:* showing the overlay of both the drug and metabolite. Data is normalised by TIC. Pixel size at 50 μm.

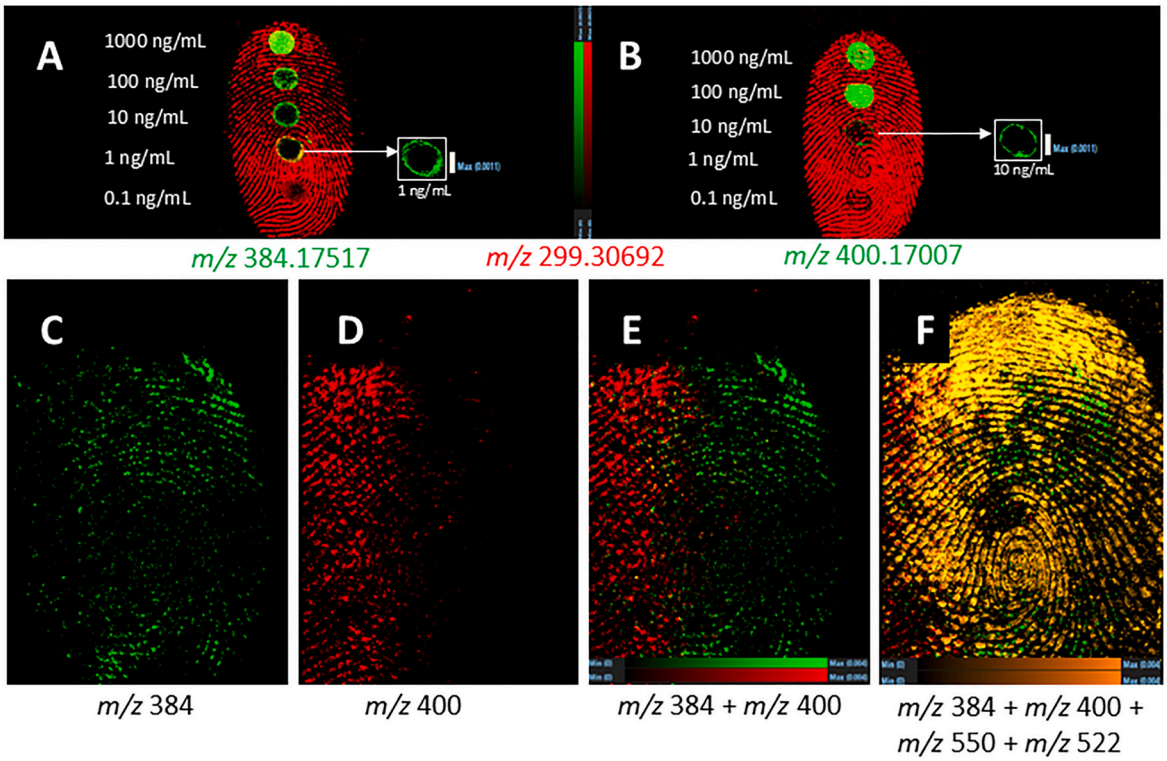


**Fig. 9.** Application of the optimised small molecules MALDI MSI method to quetiapine (*m/z* 384.17517) and 7-hydroxyquetiepine (*m/z* 400.17007) in fingerprints. *A* and *B:* sensitivity test for quetiapine and metabolite by spotting them in multiple 10-fold serial dilutions from 1000 ng/mL to 0.1 ng/mL; the images for these ions are overlaid with a fingerprint ion image at *m/z* 299.30692. *C*: MALDI MSI of fingerprints contaminated with a 1:1 mixture of quetiapine and *D* 7-hydroxyquetiapine contaminated fingerprints; *E:* shows the overlay of both the drug and metabolite, and *F:* shows the further overlay of the ions at *m/z* 550.63031 and *m/z* 522.59814 for the purpose of a better-quality ridge pattern. Data is normalised by TIC. Pixel size at 50 μm.

golden standard methods.

The aforementioned study by Ming and Heathcote [37] detected clozapine and *N*-desmethylclozapine in the sera of 20 schizophrenic patients, following a therapeutic dosage of 600 mg/day, in a range between 32.27 ng/mL (in one instance <10 ng/mL) and 1147.37 ng/mL for clozapine and 49.45 ng/mL (in one instance <10 ng/mL) and 1402.26 ng/mL for *N*-desmethylclozapine using UPLC-Tandem MS. In a more recent study by Longman et al. [26], clozapine (and to a lesser extent *N*-desmethylclozapine) were detected in the fingerprints of medicated patients, indicating for the first time that these species are excreted through sweat and specifically sweat from fingertips, even for patients dosed with as little as 25 mg/day clozapine (normal range is between 150 and 300 mg/day [38]), thus fully justifying method development to detect and image *in situ* both the drug and the metabolite in fingerprints, as presented in this paper.

In 2009, quietipine was quantified in patients' plasma at a concentration as low as 1 ng/mL. Quetiapine and 7- hydroxyquetiapine were quantified also in patients' hair at concentrations between 0.35 ng/mg to 10.21 ng/mg hair, and between 0.02 ng/mg to 3.19 ng/mg hair, respectively [39] with ratios varying between 0.97 and 13. Finally, quetiapine and 7-hydroxyquetiepine were detected in fingerprints of patients medicated in a range between 100 and 500 mg/day [26] or dosed at 300 and 600 mg/day [40], but in these studies, no quantification data were reported.

In MALDI MSI experiments, clozapine, quetiapine and their primary metabolites were imaged and detected directly in a drug-contaminated fingerprint with no prior extraction. As such, considering the fingerprint area of ~261.2 $mm^2$, and the concentrations and volumes of the two species employed (10 μg/mL, 50 μL), both clozapine and quetiapine have been visualised at an over-estimated "density" of ~1.9 ng/$mm^2$.

Whilst not directly comparable with the quantification data in the literature and reported earlier, the sensitivity achieved for the detection and imaging of both clozapine and quetiapine (and their metabolites) via MALDI MSI is considered relevant and enabling detection and mapping of these species in physiological concentrations and ratios with their metabolites.

## 4. Conclusion

This study illustrates the systematic tuning of parameters to develop an optimal MALDI-MS imaging method for small molecules using one of the latest technological developments, namely the multi-reflection device as incorporated by the SELECT SERIES MALDI-MRT. Molecular fingerprinting, specifically drug imaging in latent fingerprints has been used as case study and, for the first time clozapine and quietapine along with their metabolites have been imaged in a fingerprint in physiological ratios and abundance.

This study was prompted by both the need to expand the applications to fingerprint molecular analysis and the necessary optimisation of this new system which affords enhanced mass accuracy and spatial resolution.

Herein, the authors reported the effects and the benefits of selecting the most appropriate acquisition settings, laser and source parameters, selecting appropriate quadrupole profiles, exploring the MALDI gas and transfer collision gas parameters as well as RF parameters in order in a step-wise approach in order to maximise sensitivity and spatial resolution for small molecule imaging. This study therefore offers guidance to a systematic approach for method optimisation and provides the readers with a better understanding of this technology to maximise the information sought in their small molecule MALDI-MSI applications and a framework to accelerate method development. Importantly, The general guiding principles illustrated and underpinning understanding are

transferable/applicable to other instrumentation and applications. Further optimisation may be achieved by studying the interplay of different variables in the same analytical instance and will be considered in our laboratory in future investigations.

## CRediT authorship contribution statement

**Rohith Krishna:** Writing – review & editing, Writing – original draft, Visualization, Validation, Investigation, Formal analysis. **James Langridge:** Writing – review & editing, Supervision. **Emmanuelle Claude:** Writing – review & editing, Supervision. **Robert Bradshaw:** Writing – review & editing, Supervision. **Laura Cole:** Writing – review & editing, Supervision. **Simona Francese:** Writing – review & editing, Writing – original draft, Supervision, Methodology, Funding acquisition, Conceptualization.

## Data Statement

All data are available on request to the corresponding author s.francese@shu.ac.uk.

## Funding

This work was supported as part of a PhD Transforming Lives PhD studentship awarded by Sheffield Hallam University and co-funded by Waters Corporation, UK.

## Declaration of competing interest

The authors declare the following financial interests/personal relationships which may be considered as potential competing interests: Rohith Krishna reports financial support was provided by Waters Corporation (part-funded Rohith's PhD studentship salary). Simona Francese reports a relationship with Waters Corporation that includes: funding grants (supporting the PhD programme of which the paper represents a small part). If there are other authors, they declare that they have no known competing financial interests or personal relationships that could have appeared to influence the work reported in this paper.

## Appendix A. Supplementary data

Supplementary data to this article can be found online at https://doi.org/10.1016/j.aca.2025.343998.

## Data availability

Data will be made available on request.

## References

[1] B. Spengler, M. Hubert, R. Kaufmann, Poster Appli LAMMA 2000 ASMS94 arrangiert.pdf (uni-giessen.de). 42nd Annual Meeting of the American Society for Mass Spectrometry, 1994. (Accessed 6 March 2024).
[2] R.M. Caprioli, T.B. Farmer, J. Gile, Molecular imaging of biological samples: localization of peptides and proteins using MALDI-TOF MS, Anal. Chem. 69 (1997) 4751–4760, https://doi.org/10.1021/ac970888i.
[3] S.D. Pringle, K. Giles, J.L. Wildgoose, J.P. Williams, S.E. Slade, K. Thalassinos, J. H. Scrivens, An investigation of the mobility separation of some peptide and protein ions using a new hybrid quadrupole/travelling wave IMS/oa-ToF instrument, Int. J. Mass Spectrom. 261 (2007) 1–12, https://doi.org/10.1016/j.ijms.2006.07.021.
[4] K. Giles, S.D. Pringle, K.R. Worthington, D. Little, J.L. Wildgoose, R.H. Bateman, Applications of a travelling wave-based radio-frequency-only stacked ring ion guide, Rapid Commun. Mass Spectrom. 18 (2004) 2401–2414, https://doi.org/10.1002/rcm.1641.
[5] K. Giles, J. Ujma, J. Wildgoose, S.D. Pringle, K. Richardson, D. Langridge, M. Green, A cyclic ion mobility-mass spectrometry system, Anal. Chem. 91 (2019) 8564–8573, https://doi.org/10.1021/acs.analchem.9b01838.
[6] M.A. Park, Apparatus and method for parallel flow ion mobility spectrometry combined with mass spectrometry, US Pat. 8 (2010) 288–717.
[7] F. Fernandez-Lima, D.A. Kaplan, M.A. Park, Integration of trapped ion mobility spectrometry with mass spectrometry, Rev. Sci. Instrum. 82 (2011) 126106, https://doi.org/10.1063/1.3665933.
[8] M.E. Ridgeway, M. Lubeck, J. Jordens, M. Mann, M.A. Park, Trapped ion mobility spectrometry: a short review, Int. J. Mass Spectrom. 425 (2018) 22–35, https://doi.org/10.1016/j.ijms.2018.01.006.
[9] LCMS-173, The combination of MALDI-2 and timsTOF fleX brings targeted drug imaging to the next level, Application Note. https://www.bruker.com/en/meta/fileadmin.html?q_1=LCMS%2520173, 2020. (Accessed 12 September 2024).
[10] F.P.Y. Barré, M.R.L. Paine, B. Flinders, A.J. Trevitt, P.D. Kelly, R. Ait-Belkacem, J. P. Garcia, L.B. Creemers, J. Stauber, R.J. Vreeken, B. Cillero-Pastor, S.R. Ellis, R.M. A. Heeren, Enhanced sensitivity using MALDI imaging coupled with laser post-ionization (MALDI-2) for pharmaceutical research, Anal. Chem. 91 (2019) 10840–10848, https://doi.org/10.1021/acs.analchem.9b02495.
[11] FlashNote-12 - Caution, MALDI-2 detects analyte classes never seen before (lcms.cz) Application Note. https://lcms.labrulez.com/paper/7559, 2020. (Accessed 12 September 2024).
[12] J. Soltwisch, B. Heijs, A. Koch, S. Vens-Cappell, J. Höhndorf, K. Dreisewerd, MALDI-2 on a trapped ion mobility quadrupole time-of-flight instrument for rapid mass spectrometry imaging and ion mobility separation of complex lipid profiles, Anal. Chem. 92 (2020) 8697–8703, https://doi.org/10.1021/acs.analchem.0c01747.
[13] MS Imaging – The SELECT SERIES™ MALDI and MRT, Waters Corp. application note. https://www.waters.com/webassets/cms/library/docs/720007652en.pdf. (Accessed 10 September 2024).
[14] F. Barré, B. Rocha, F. Dewez, M. Towers, P. Murray, E. Claude, B. Cillero-Pastor, R. M.A. Heeren, T.P. Siegel, Faster raster matrix-assisted laser desorption/ionization mass spectrometry imaging of lipids at high lateral resolution, Int. J. Mass Spectrom. 437 (2019) 38–48, https://doi.org/10.1016/j.ijms.2018.09.015.
[15] S. Francese, C. Heaton, Emerging technologies: use of matrix-assisted laser desorption ionization mass spectrometry for the analysis of fingermark and blood evidence, in: Applications of Mass Spectrometry for the Provision of Forensic Intelligence: State-Of-The-Art and Perspectives, RSC, 2023, pp. 159–183.
[16] S. Francese, S.M. Bleay, Applications of Mass Spectrometry for the Provision of Forensic Intelligence—State of the Art and Perspectives, RSC, Cambridge, 2023.
[17] H. Bandey, V. Bowman, S. Bleay, R. Downham, V.H. Sears, in: H. Bandey (Ed.), Fingermark Visualization Manual, CAST, Home Office, Sandridge, UK, 2014.
[18] H. Bandey, Fingermark Visualization Manual, second ed., 2023. Dstl: Salisbury, UK.
[19] G. Groeneveld, M. de Puit, S. Bleay, R. Bradshaw, S. Francese, Detection and mapping of illicit drugs and their metabolites in fingermarks by MALDI MS and compatibility with forensic techniques, Sci. Rep. 5 (2015) 11716, https://doi.org/10.1038/srep11716.
[20] M.J. Bailey, et al., Rapid detection of cocaine, benzoylecgonine, and methylecgonine in fingerprints using surface mass spectrometry, Analyst 140 (2015) 6254–6259, https://doi.org/10.1039/c5an00112a.
[21] R. Bradshaw, N. Denison, S. Francese, Implementation of MALDI MS profiling and imaging methods for the analysis of real crime scene fingermarks, Analyst 142 (2017) 1581–1590, https://doi.org/10.1039/c7an00218a.
[22] K. Kaplan-Sandquist, M.A. LeBeau, M.L. Miller, Chemical analysis of pharmaceuticals and explosives in fingermarks using matrix-assisted laser desorption ionization/time-of-flight mass spectrometry, Forensic Sci. Int. 235 (2014) 68–77, https://doi.org/10.1016/j.forsciint.2013.11.016.
[23] R. Bradshaw, R. Wolstenholme, R.D. Blackledge, M.R. Clench, L.S. Ferguson, S. Francese, A novel matrix-assisted laser desorption/ionization mass spectrometry imaging-based methodology for the identification of sexual assault suspects, Rapid Commun. Mass Spectrom. 25 (2011) 415–422, https://doi.org/10.1002/rcm.4858.
[24] R. Wolstenholme, R. Bradshaw, M.R. Clench, S. Francese, Study of latent fingermarks by matrix-assisted laser desorption/ionisation mass spectrometry imaging of endogenous lipids, Rapid Commun. Mass Spectrom. 23 (2009) 3031–3039, https://doi.org/10.1002/rcm.4218.
[25] V.G. Masdrakis, D.S. Baldwin, Prevention of suicide by clozapine in mental disorders: systematic review, Eur. Neuropsychopharmacol. 69 (2023) 4–23, https://doi.org/10.1016/j.euroneuro.2022.12.011.
[26] K. Longman, C. Frampas, H. Lewis, C. Costa, R. Nilforooshan, M. Chambers, M. Bailey, Non-invasive drug adherence monitoring of antipsychotic patients via finger sweat testing, Front. Chem. 11 (2023) 1245089, https://doi.org/10.3389/fchem.2023.1245089.
[27] Y. Hsieh, R. Casale, E. Fukuda, J. Chen, I. Knemeyer, J. Wingate, R. Morrison, W. Korfmacher, Matrix-assisted laser desorption/ionization imaging mass spectrometry for direct measurement of clozapine in rat brain tissue, Rapid Commun. Mass Spectrom. 20 (2006) 965–972, https://doi.org/10.1002/rcm.2397.
[28] K. Robichon, S. Sondhauss, T.W. Jordan, et al., Localisation of clozapine during experimental autoimmune encephalomyelitis and its impact on dopamine and its receptors, Sci. Rep. 11 (2021) 2966, https://doi.org/10.1038/s41598-021-82667-6.
[29] P. Willis, J. Jaloszynski, V. Artaev, Improving duty cycle in the Folded Flight Path high-resolution time-of-flight mass spectrometer, Int. J. Mass Spectrom. 459 (2021) 116467.
[30] M. Towers, E. Claude, M. Palmer, D.C. Shepherd, S. Lai, High resolution imaging platform incorporating MALDI and DESI. https://www.waters.com/waters/library.htm?locale=186&lid=135131943&cid=511436, 2022. (Accessed 7 August 2024).
[31] P. Trim, M. Djidja, S.J. Atkinson, K. Oakes, L.M. Cole, D.M.G. Anderson, P.J. Hart, S. Francese, M.R. Clench, Introduction of a 20 kHz Nd laser into a hybrid quadrupole time-of-flight mass spectrometer for MALDI-MS imaging, Anal.

Bioanal. Chem. 397 (2010) 3409–3419, https://doi.org/10.1007/s00216-010-3874-6.
[32] H. Kettling, S. Vens-Cappell, J. Soltwisch, A. Pirkl, J. Haier, J. Müthing, K. Dreisewerd, MALDI mass spectrometry imaging of bioactive lipids in mouse brain with a Synapt G2-S mass spectrometer operated at elevated pressure: improving the analytical sensitivity and the lateral resolution to ten micrometers, Anal. Chem. 86 (2014) 7798–7805, https://doi.org/10.1021/ac5017248.
[33] J.C. McKinnon, H.H. Milioli, C.A. Purcell, C.L. Chaffer, B. Wadie, T. Alexandrov, T. W. Mitchell, S.R. Ellis, Enhancing metabolite coverage in MALDI-MSI using laser post-ionisation (MALDI-2), Anal. Methods 15 (2023) 4311–4320, https://doi.org/10.1039/d3ay01046e.
[34] K. Dreisewerd, The desorption process in MALDI, Chem. Rev. 103 (2) (2003) 395–426.
[35] S.J. Wetzel, C.M. Guttman, K.M. Flynn, J.J. Filliben, Significant parameters in the optimization of MALDI-TOF-MS for synthetic polymers, J. Am. Soc. Mass Spectrom. 17 (2006) 246–252, https://doi.org/10.1016/j.jasms.2005.11.007.
[36] B.M. Prentice, D.J. Ryan, R. Van de Plas, R.M. Caprioli, J.M. Spraggins, Enhanced ion transmission efficiency up to m/z 24,000 for MALDI protein imaging mass spectrometry, Anal. Chem. 90 (2018) 5090–5099, https://doi.org/10.1021/acs.analchem.7b05105.
[37] D.S. Ming, J. Heathcote, Therapeutic drug monitoring of clozapine and norclozapine in human serum using ultra-performance liquid chromatography-tandem mass spectrometry, J. Anal. Toxicol. 33 (2009) 198–203, https://doi.org/10.1093/jat/33.4.198.
[38] S. Subramanian, B.A. Völlm, N. Huband, Clozapine dose for schizophrenia, Cochrane Database Syst. Rev. 6 (2017), https://doi.org/10.1002/14651858.CD009555.
[39] T.M. Binz, M. Yegles, S. Schneider, H. Neels, C.L. Crunelle, Time resolved analysis of quetiapine and 7-OH-quetiapine in hair using LC/MS–MS, Forensic Sci. Int. 242 (2014) 200–203, https://doi.org/10.1016/j.forsciint.2014.07.002.
[40] C. Costa, C. Frampas, K.A. Longman, V. Palitsin, M. Ismail, P. Sears, R. Nilforooshan, M.J. Bailey, Paper spray screening and liquid chromatography/mass spectrometry confirmation for medication adherence testing: a two-step process, Rapid Commun. Mass Spectrom. 35 (2021) e8553, https://doi.org/10.1002/rcm.8553.